CHAPTER - 5

Study of Cerium doped Cadmium Tungstate at different pH

5.1. Introduction

Metal tungstates have good application prospects in scintillators, optical fibers, microwave applications, humidity sensors, photoluminescence materials etc., [1-4]. Cadmium tungstate ($CdWO_4$) have been investigated for many applications, such as, oil well logging, industrial processing control and inspection, dosimetry, and nuclear weapons and waste monitoring [5-9].

Hydrothermal synthesis of these materials by the synthetic route is a simple and cost effective method that provides a high yield with easy scale up. This method is emerging as a viable alternative approach for the synthesis of inorganic materials with appropriate choice of experimental parameters, such as temperature, time, pH, mineralizer and surfactant. It offers several advantages over other synthesis process, such as mild experimental conditions, high purity, and good particle size distribution of product.

The tungstates doped with rare-earth nanophosphors have attracted special attention compared to the corresponding bulk materials which have large practical applications in solid state lighting and displays. In the present work, we report the synthesis of cerium doped $CdWO_4$ by hydrothermal method. It is noticed that the pH of solution plays an essential role in crystal growth under hydrothermal conditions [9,11]. Liao et al. [12] examined the effect of the wide pH of synthesizing solution on the formation of $CdWO_4$ nanorods and reported an optimal range of the initial pH value to be 3 to 8. Recently, Mirabbos et al. [13] investigated the effect of the pH of synthesizing

solution on the formation of besom-like $CdWO_4$ structures.

The present chapter reports synthesis, structural and optical studies of Cerium doped Cadmium tungstate with different pH by hydrothermal method. The received materials are characterized by PL, XRD, TEM and FTIR.

5.2. Sample Preparation

Cadmium Chloride ($CdCl_2 .H_2O$), Sodium Tungstate ($Na_2WO_4.2H_2O$) and Cerium Oxide (CeO_2) of analytical grade were used as received without any further purification purchased from Alfa Aesar. Distilled water was used as a solvent to prepare all required solutions used in the present investigations. Initially 40 ml solution of 0.1M concentration of $CdCl_2.H_2O$ was prepared by continuous stirring and also 40 ml solution of 0.1M concentration of $Na_2WO_4.2H_2O$ was added into it drop wise subsequently 40 ml solution of 0.01M concentration of CeO_2 was added. The pH value 4 and 6 of this solution was adjusted drop wise with CH_3COOH solution.. The pH value 8 of this solution is adjusted by NaOH solution. These precursor solutions were transferred to Teflon fitted stainless-steel autoclave having 150 ml capacity filled with reaction media up to 80% one by one. The autoclave was maintained at a temperature of 150^oC for 12 h and allowed to cool to room temperature. The prepared samples were washed several times with distilled water and lastly washed with absolute ethanol. A white powder was obtained after drying in vacuum at 80^oC for 2 hours.

5.3 X-Ray Diffraction (XRD) – Structural Study

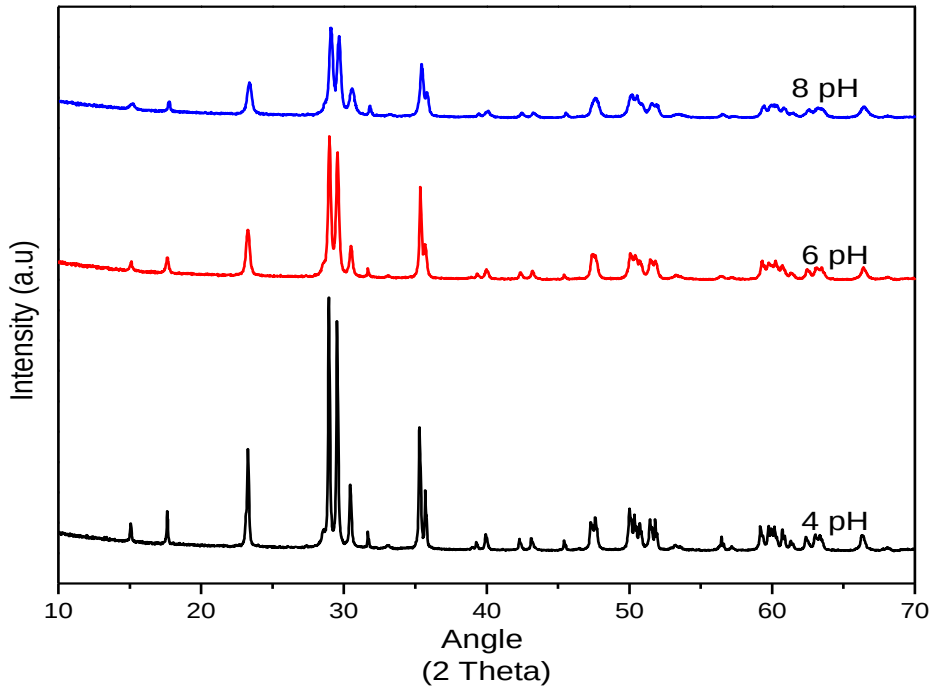

Figure 5.1 XRD patterns of Cerium doped $CdWO_4$ synthesized at pH (4, 6, 8)

Figure 5.1 shows the XRD patterns of $CdWO_4$:Ce powders prepared at different pH (4, 6, 8).XRD patterns revealed that the $CdWO_4$ can be indexed to a pure monoclinic phase of $CdWO_4$ with a wolframite structure with space group P2/c (13) ; in agreement with JCPDS (Joint Committee on Powder Diffraction Standards) card No. 14-0676. It can be seen that the crystal structures of all the samples belong to the pure monoclinic phase. However, by comparing the curves of the three products, it is observed that the relative intensity of the peaks varied considerably, which indicates different crystallinity. The samples prepared at pH 4 and 6 show better crystallization than the one made at pH 8. The broadening of the peaks indicates that the crystallite size is small. These XRD

patterns indicate that well-crystallized $CdWO_4$ crystals were observed in the current synthetic process. This result shows that different pH supports the formation of crystalline $CdWO_4$ nanostructures at low synthesis temperature therefore reduces the processing time than other conventional methods.

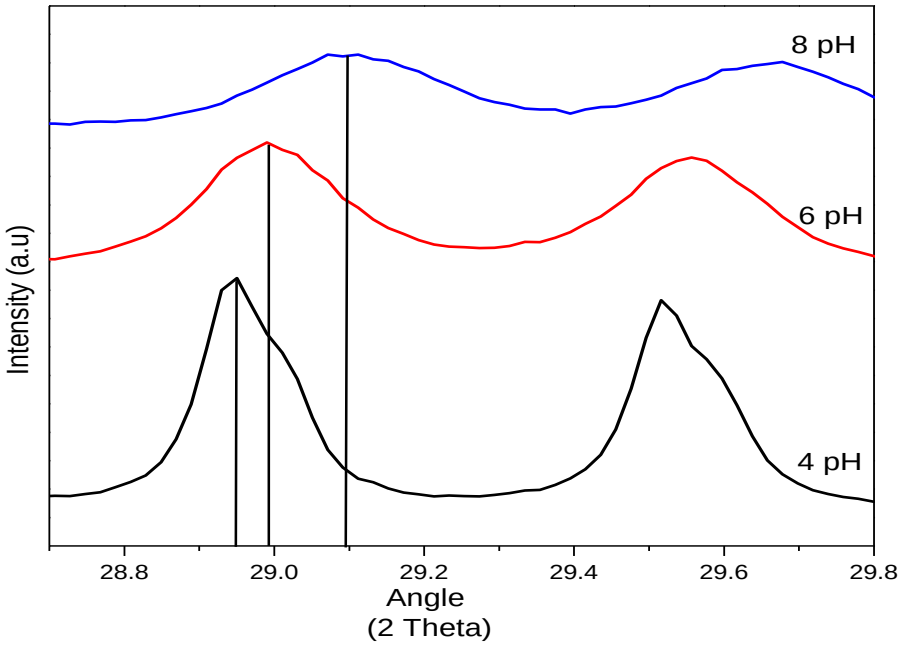

Figure 5.1a Shift of reflection peak of Cerium doped $CdWO_4$ synthesized at pH (4, 6, 8).

Shift in the main reflection peak of $CdWO_4$ is compared and presented in Figure 5.1a. It can be seen from the figure that when sample prepared at 4 pH is at lowest angle and that for sample prepared at 8 pH is at highest angle. According to the Bragg equation, the shift toward higher angle of reflection suggests that the cell parameters of as-synthesized products could continuously decrease and also crystallite size decreases.

pH	Lattice parameters (Å)			Volume (Å ^{3})	Avg. crystallite size(nm)
	a	B	C		
4	5.0240	5.865	5.0860	150.66	55
6	5.0280	5.8620	5.0670	150.30	47
8	5.0110	5.8040	5.0500	149.78	44

Table 5.1 Lattice parameters and average crystallite size

The summary of lattice parameters and average crystallite size calculated using the Scherrer formula are given table 5.1.

$$D = \frac{k\lambda}{\beta cos\theta}$$

Where D is the average crystallite size, k is the constant equal to 0.89, λ is the wavelength of the X-rays equal to 0.1542 nm and β is FWHM.

From the table 5.1 the calculated cell volumes and crystallite size of Cerium doped $CdWO_4$ continuously decreases as the pH increases. The calculated crystallite size using XRD data suggest that the prepared $CdWO_4$ are in nanosize.

5.4 Photoluminescence (PL) Study

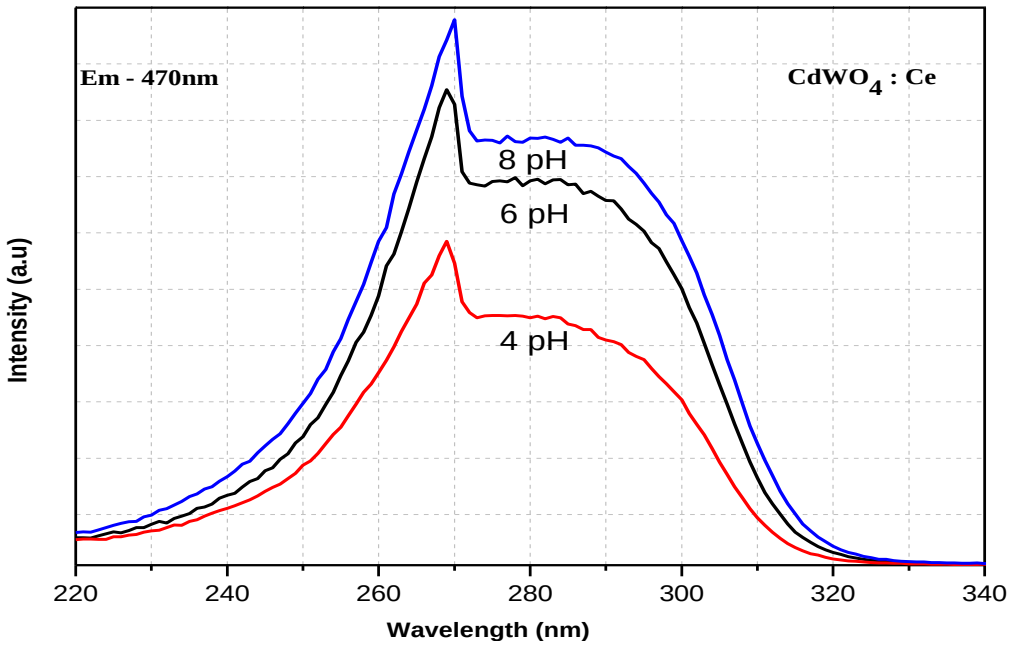

Figure 5.2 Excitation spectra of Cerium doped $CdWO_4$ synthesized at pH (4, 6, 8).

The excitation spectra of Ce doped $CdWO_4$ phosphors recorded at room temperature is shown in Fig. 5.2 when monitored at 470nm. Broad absorption band was observed between 240 nm and 320 nm. The absorption intensity of the broad band centered on 270nm increases when the pH increases from 4 to 8. The intensity is more than 50% increase when compared 8pH to 4pH.

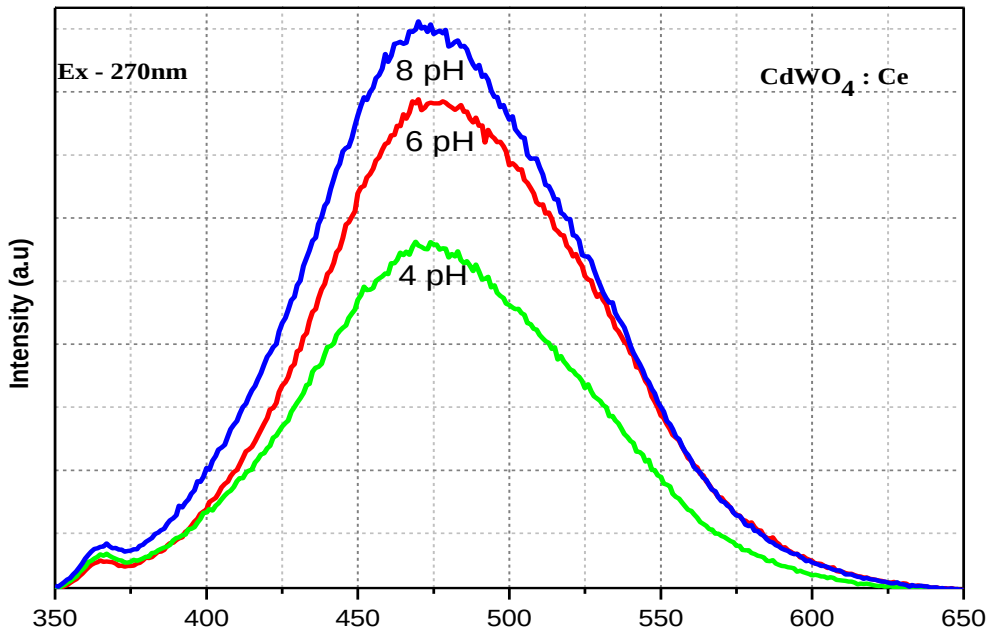

Figure 5.3 PL Emission spectra of Cerium doped $CdWO_4$ synthesized at pH (4, 6, 8).

Phosphor	pH	Excitation wavelength (nm)	Excitation energy (eV)	Peak position (nm)	Peak emission energy (eV)	Peak Intensity (a.u.)
$CdWO_4$:Ce	4			476	2.60	421
	6	270	4.59201	476	2.60	591
	8			469	2.64	685

Table 5.2 PL Emission spectra analysis of Cerium doped $CdWO_4$ synthesized at pH (4, 6, 8)

The PL spectra of the Cerium doped $CdWO_4$ synthesized at different pH are shown in

Fig. 5.3. It is clearly seen that, the PL emission band (380-600 nm) with intense emission (469 nm and 476 nm) are identical in all three spectra. The low intensity peaks at 368 nm; in near-UV region is also observed in all three spectra. The results indicate that PL spectra exhibit violet - green emission band peaking in blue region with a band edge UV emission. The emission bands were ascribed to the $^1A_1 \rightarrow {}^3T_1$ transition within the WO_6^{6-} complex [14]. This is mainly due to the charge-transfer transitions between the O_{2p} orbital and the empty d orbital of the central W^{6+} of WO_6 octahedra or to the self-trapped exciton at a WO_6^{6-} oxyanion complex [15,16]. The band edge UV emission may be due to recombination of free excitons through in exciton-exciton collision process or the radiative recombination of excitons bound to neutral donor and also due to crystal filed [17,18]. The change in PL intensity can be attributed to change in dimensional confinement of Ce ions which is due to the preparation of the material through effective approach of varying pH.

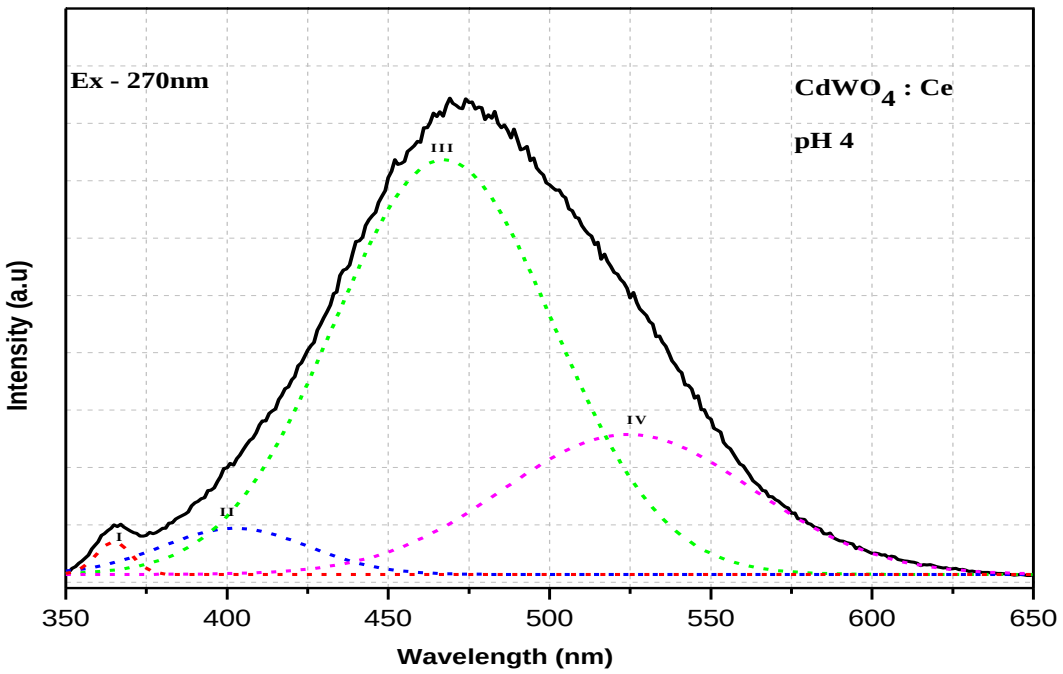

Figure 5.4a Gaussian peaks of Cerium doped $CdWO_4$ with 4 pH.

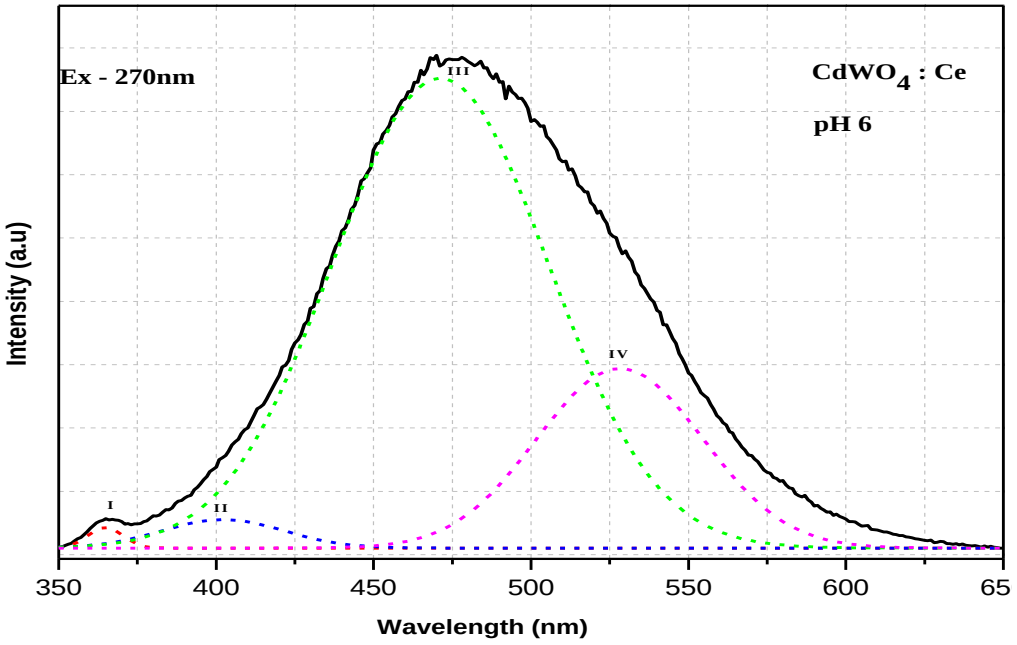

Figure 5.4b Gaussian peaks of Cerium doped $CdWO_4$ with 6 pH.

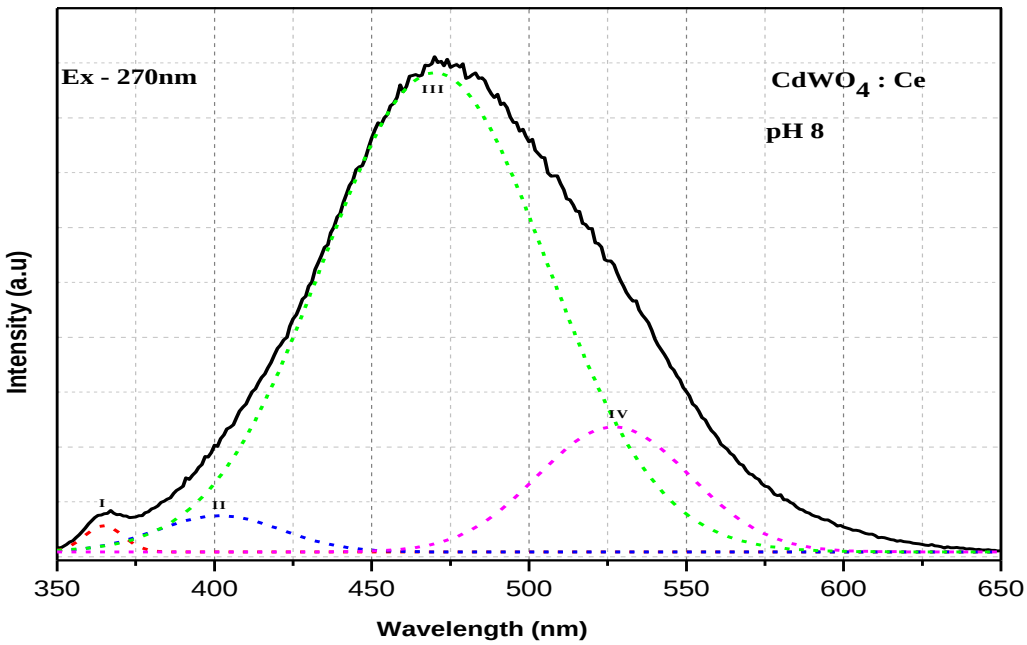

Figure 5.4c Gaussian peaks of Cerium doped $CdWO_4$ with 8 pH.

Sample	pH	Gaussian peak I		Gaussian peak II		Gaussian peak III		Gaussian peak IV	
		Intensity	Wavelength	Intensity	Wavelength	Intensity	Wavelength	Intensity	Wavelength
$CdWO_4$:Ce	4	35	365	47	402	368	468	129	526
$CdWO_4$:Ce	6	32	365	41	405	563	471	220	527
$CdWO_4$:Ce	8	42	365	56	401	661	471	177	527

Table 5.3 Position of Gaussian peak of PL spectra of Cerium doped $CdWO_4$ with different pH.

As we can see from the PL spectra within the range of pH 4 to 8, the position of the emission peaks of the phosphor remained almost unchanged for all the samples. In order to obtain the detailed parameters about the luminescence of $CdWO_4$, Gaussian

fitting was done for four individual lines to achieve good agreement with the experimental data which is shown in Figure 5.4(a,b,c). Variation in the position of Gaussian peaks with their intensity is shown in Table 5.3.

The Gaussian peak I and Gaussian peak II are observed in UV and violet region respectively. The Gaussian peak III observed in blue region and it is characteristic band of tungstate. This band was ascribed to the $^1A_1 \rightarrow {}^3T_1$ transition within the WO_6^{6-} complex [14]. This is mainly due to the charge-transfer transitions between the O_{2p} orbital and the empty d orbital of the central W^{6+} of WO_6 octahedra or to the self-trapped exciton at a WO_6^{6-} oxyanion complex [19, 20].

The Gaussian peak IV corresponds to green emission which is assumed to arise from oxygen deficient regular WO_3 group also called 'F' center. Oxygen vacancies VO (or F++) can capture one or two electrons from $[WO_4^{2-}]$ to form 'F+' or 'F' centers and so $[WO_4^{2-}]$ is changed into WO_3. This emission as a result of the photo-thermally stimulated disintegration of localized exciton states and subsequent recombination of the produced electron and hole centers near WO_3 groups. This emission also ascribed to intrinsic luminescence probably originates from localized exciton in octahedral WO_6^{6-} groups in the wolframite phase.

According to XRD data, sample prepared with 8pH has highest crystallinity and sample prepared with 4pH has lowest crystallinity. It indicates that PL spectra of nano-sized $CdWO_4$ crystallites are strongly relied on their particle size and crystallinity. PL intensity has direct relation with crystallinity. The better crystallinity, the higher PL emission peak is of $CdWO_4$ obtained at 8 pH. However, the absolute luminescence

intensity increased with increasing pH over the range of 4 to 8 pH. It exhibits that the nanorods and hollow nano tube have strong luminescence intensity. The very weak PL intensity of the sample obtained for pH 4 due to poor crystallinity.

The PL intensity of blue emission peak is highest for sample prepared at 8pH (Hollow nano tube) and lowest for sample prepared at 4pH (Nanosphere). It indicates that $CdWO_4$ hollow nano tube (HNT) have more regular lattice structure and uniform morphology compared to nanorods and nanosphere. Sample prepared at 4pH has lowest regular lattice structure. Similarly, The PL intensity of green emission peak is highest for sample prepared at 8pH (HNTs) intermediate for sample prepared at 6pH (Nanorods) and lowest for sample prepared at 4pH (Nanosphere) which indicates that $CdWO_4$ HNTs have highest defect centers relative to oxygen due to faster 1-D crystal growth compared to Nanorods and sample prepared at 4pH has lowest defect centers relative to oxygen. Size-dependent emission of photoluminescence observed between these three products with different shapes indicates that the sizes of these structures are so in the quantum confinement regime.

The intensity of PL emission spectra increases with the increase in the pH of synthesizing solution this may be due to the formation of low dimension of the materials. This leads to availability of more number of particles for the formation of the excited electrons and hole pairs. Therefore, the PL intensity depends on the morphology as well as less in dimension of the materials of $CdWO_4$ [21-23]. PL emission mainly originates from recombination of excited electrons and holes. Low PL emission intensity indicates that phosphor has a low recombination rate and high separation rate of electrons-holes as

well as large particles in nano range. In the case of 8pH, the high intensity peak is obtained due to high recombination rate and low separation rate between electrons-holes.

pH	Peak Position (nm)	Peak Intensity	Shape
4	476	421	Nanosphere
6	476	591	Nanorod
8	469	685	Hollow nano tube

Table 5.4 Peak position with respect to pH.

It is also observed from the figure 5.3 and table 5.4 that there is a minor peak shift of 7 nm which is mainly responsible due to the medium in which occupation of Ce ions in the substitution positions of $CdWO_4$ host crystal lattice. From XRD and TEM measurements, it is inferred that all the samples have same phase. Therefore, the shifting of peak does not relate with phase and it is attributed to effect of dopant in basic medium. The position of the peak changes in 8 pH solution compare to 4pH and 6pH solution and shift occurred from blue to violet region. In our earlier work [24] we reported the shift obtained due to dopant but in the present case the shift can be occurred due the formation of less volume particles in nano scale when compared to 4pH mainly due to basic preparation medium.

5.5 FTIR Studies

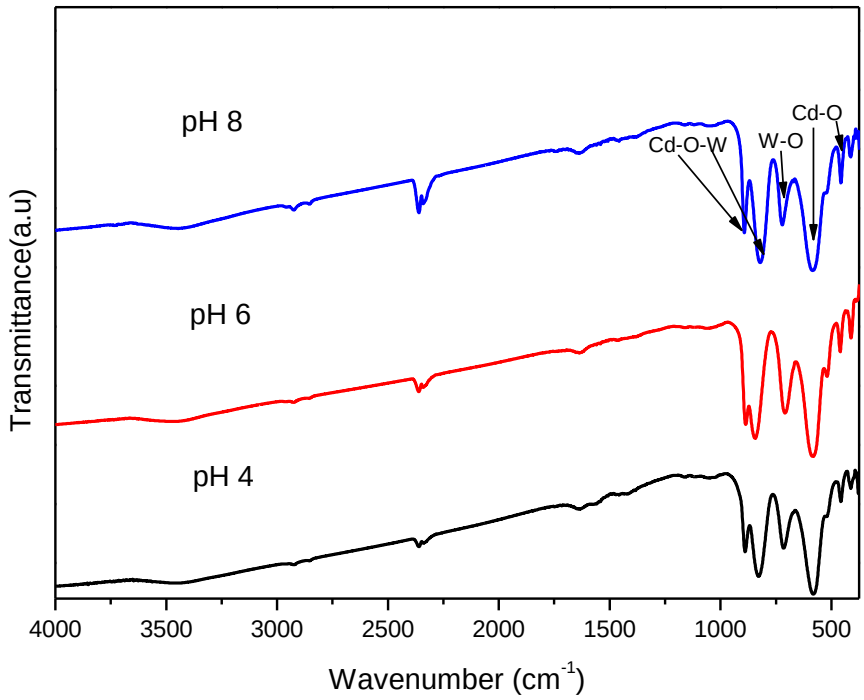

Figure 5.5 Room temperature FTIR spectra of Cerium doped$CdWO_4$ synthesized at pH(4, 6, 8).

Figure 5.5 shows FTIR spectra recorded in the range of 1600-400 cm^{-1} of the Cerium doped $CdWO_4$ particles. FTIR measurements were done using KBr method at room temperature. The intrinsic bending and stretching vibrations of Cd-O (517,560cm^{-1}), W-O (~680 cm^{-1}) and Cd-O-W (~824 cm^{-1}) were observed in the all three samples. The FTIR spectrum of all samples exhibit broad band below 710 cm^{-1} which is due to the δ (Ce-O-C) mode [25].

5.5. Transmission Electron Microscopy (TEM)

Figure 5.6 shows TEM image of cerium-doped samples of the $CdWO_4$ prepared at 150^0C for 12 h. The TEM image shows nano spheres when pH maintained at 4, the average diameter of nano sphere is around 110~150 nm. It exhibits distinct boundaries of nanospheres formed and are seen quite smooth. The nano spheres have been distributed homogenously at 4pH.

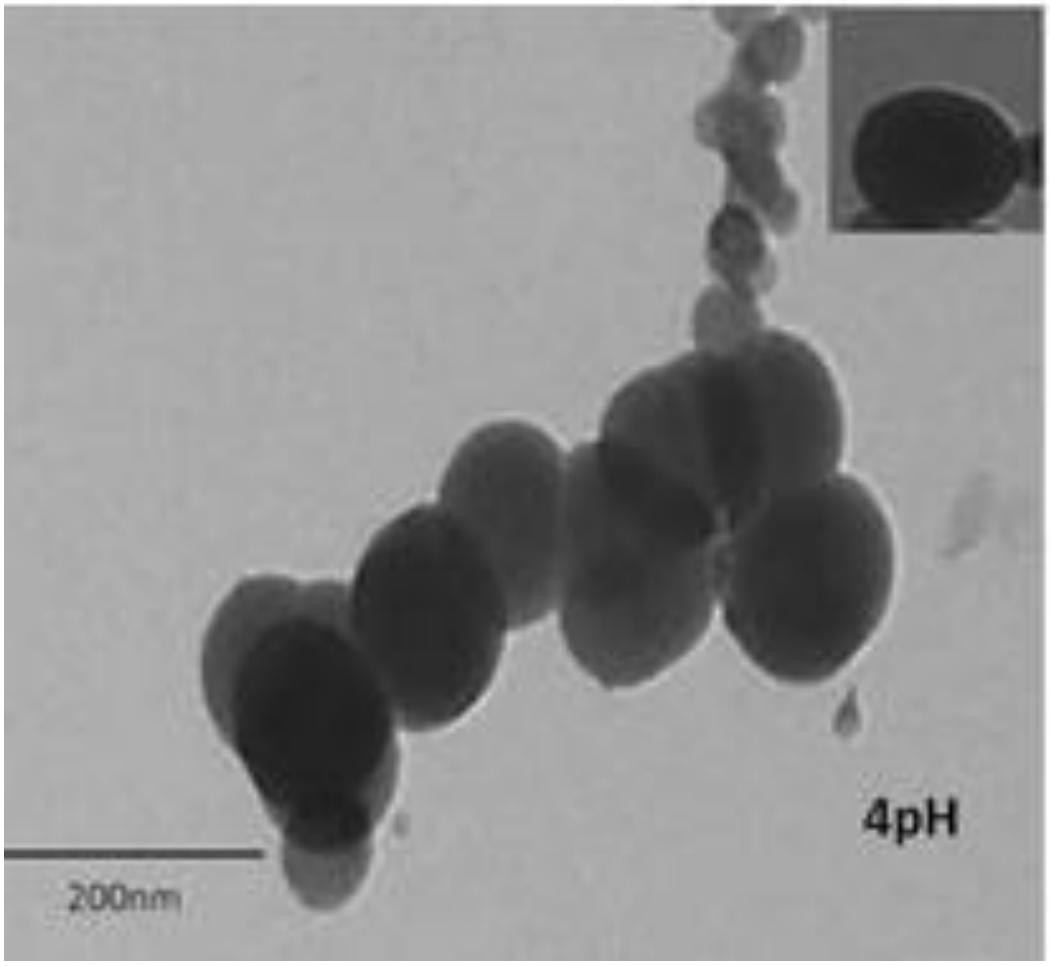

Figure 5.6 TEM images of Cerium doped$CdWO_4$synthesized at pH 4

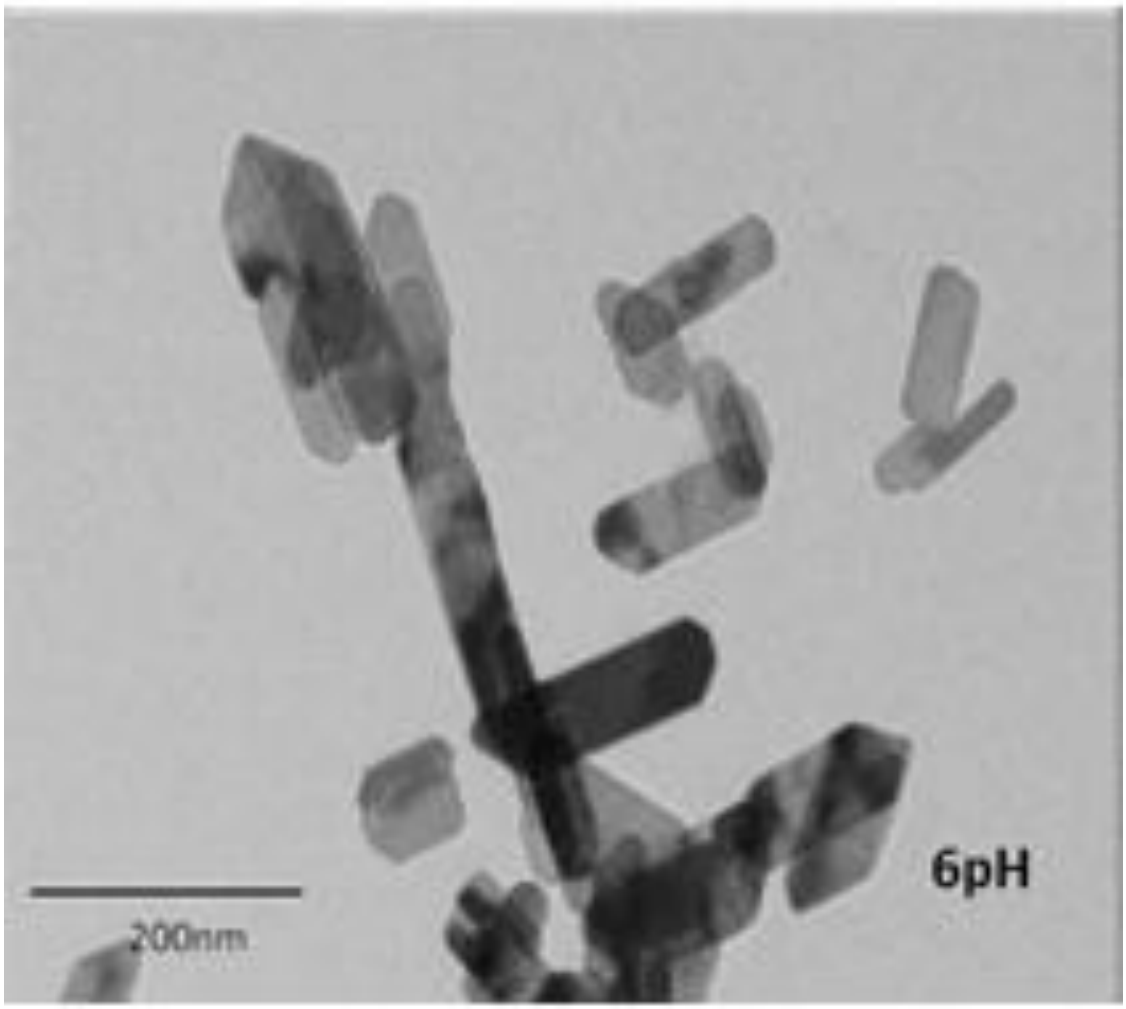

Figure 5.7 TEM images of Cerium doped$CdWO_4$synthesized at pH 6

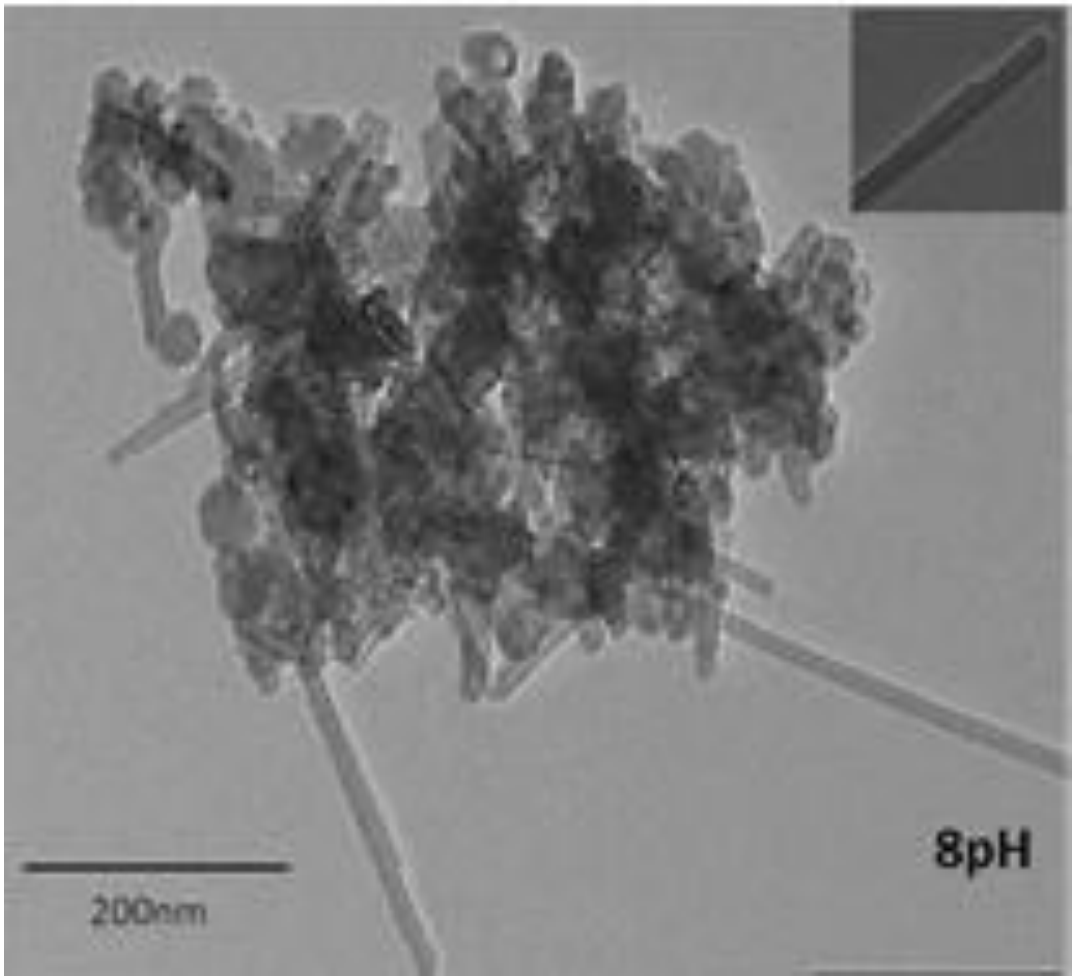

Figure 5.8 TEM images of Cerium doped$CdWO_4$ synthesized at pH 8

When the pH maintained at 6, 1-dimensional nano rods have been observed from figure 5.7. It is seen from the figure that all $CdWO_4$ nano rods are self-assembled. From the TEM figure the length of the nanorod is around 70-120 nm and the width is about 50nm for 6pH material.

Figure 5.8 shows TEM image for 8 pH material we found agglomerated particles and also hallow nanotubes. Hollow nanotubes have an average outer diameter of about 10~20 nm and their length increases from 50~300nm. From TEM for 8pH material the

shape of the particles is not perfectly spherical and also having non-uniform rough surface along with hollow nano tubes. Because of the small diameter, these nanotubes have tendency to bundle together, this phenomenon always observed in single walled carbon nanotubes. A sharp observation of the nanotubes reveals that they have a narrow width distribution and identical inner and outer diameter throughout their entire length.

Construction of hollow nanotubes in our case can be explained on the basis of Kirkendall counter diffusion effect. In this effect two solutions $CdCl_2$ (solution A) and Na_2WO_4 (solution B) sacrifice themselves to produce hollow nano tube of $CdWO_4$ (solution AB). Our group first time proposed that there are two possible approaches which are named as **Approach A** and **Approach B**. Both possibilities are based on Core/Shell model with difference only in Core and Shell Compound [26, 27]. Approach A is shown schematically in Figure 5.9 The approach A can be explained as following steps:

(I)The mechanism initiates when pH is 8.

(II) It is expected that when pH is maintained at 8, $CdCl_2$ molecule behaves as a Core and Na_2WO_4 molecule gathered around it and forms a shell.

(III) Cd^{2+} ion from the core diffuse to the shell side and WO_4^{-2} ion from the shell diffuse towards the core side. At the same time small isotropic voids will form in core contains only Cl^- ions. By this way Kirkendall diffusion will takes place in the form of two ways and corresponding mass will exchange (Wagner counter diffusion) between

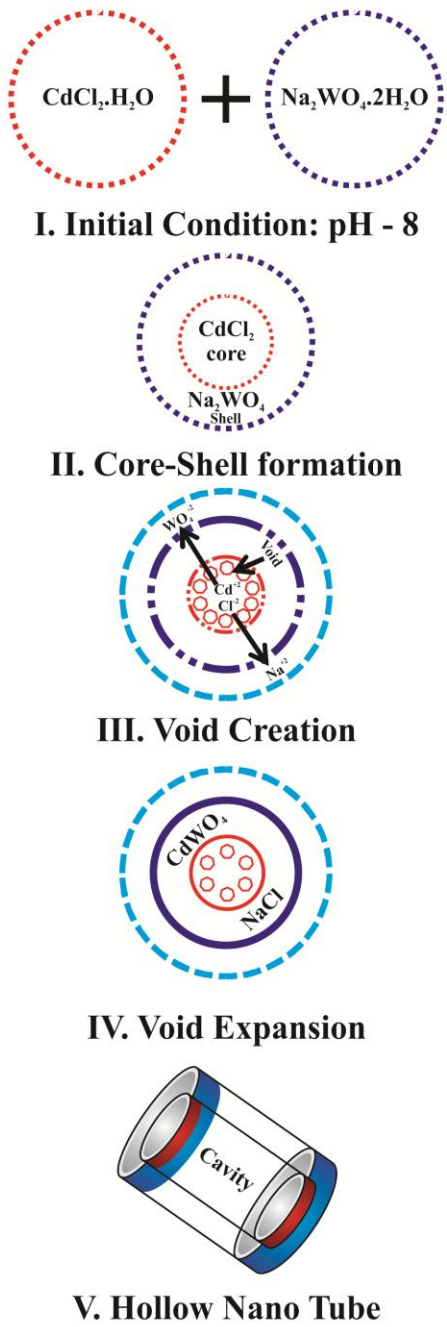

Figure 5.9 Approach A for formation of hollow nano tube.

core and shell compounds. Thus, the product $CdWO_4$ forms at the edge of the core/shell interface site. Simultaneously, Na^+ move and react with Cl^- at outer side to form NaCl which may be dissolved in generated aqueous solution.

(IV) Small voids fuse into each other and forms larger voids.

(V) By this approach, hollow nano tubes will be produced with larger cavity.

Hollow nano tube of $CdWO_4$ may also be formed via Approach B which is in a similar way by considering $Na2WO_4$ as Core and $CdCl_2$ as Shell.

The main formation of hollow nano tube is due to the change in nature of aqueous solution from acidic to basic where the pH was changed from 4 to 8. The mechanism of the $CdWO_4$ nanorods through hydrothermal approach shows that the growth process is not assisted by surfactant or template-directed, As no surfactants or templates are introduced into the synthesis process, it is confirmed from our result, that the increase in pH affects the corresponding change in size of $CdWO_4$ nanoparticles as well as length of the $CdWO_4$ nanotubes and nanorods.

Form the above study, we conclude that Cerium doped $CdWO_4$ was successfully synthesized by hydrothermal process for 4, 6 and 8 pH. XRD patterns reveal that the cell parameters of as-synthesized products could continuously decrease and also crystallite size decreases as pH increases. TEM images infer that pH affect the morphology of cadmium tungstate in terms of its shape and size. PL emission studies shows broad intense peak at 469 nm and 476 nm wavelength at 270 nm excitation wavelength in violet - green region peaking in blue region due the formation of low dimensional particles in nano scale . It suggest that more radiative traps generate in basic preparative medium

when compare to acidic solution and shifting of peak is attributed to basic medium due the formation of particles having least volume in nano scale.

The following conclusions are drawn from this chapter are given as below:

Cerium doped $CdWO_4$ phosphor has been successfully using varying pH in hydrothermal method.

From the XRD studies, it is concluded that as pH varies the cell volume and crystallite size reduced marginally.

As pH increases from 4 to 8, the PL intensity of characteristic peak increases more than 60 percentages. The increase in intensity is attributed to hollow nano tube which is confirmed by TEM studies. Since the hollow nano tubes are present where phosphors are prepared at 8 pH, it reflects that the coloumbic repulsion are minimum which leads increase in intensity of characteristic peak of $CdWO_4$.

From TEM studies, it is inferred that as pH increases 4 to 8, the phosphors change their shapes from spheres to rods and hollow tubes where all are in pure nano scale. Therefore, it is emphasized and concluded that the hydrothermal process can be adopted to synthesize or prepare the custom required nano material by varying pH.

References

1. S.J. Chen, J.H. Zhou, X.T. Chen, J. Li, L.-H. Li, J.-M. Hong, Z.L. Xue, X.-Z. You, Chem. Phys. Lett. 375, 185, 2003.
2. S. Kwan, F. Kim, J. Akana, Chem. Comm, 447, 2001.
3. B. Liu, S.-H. Yu, F. Zhang, L.J. Li, Q. Zhang, L. Ren, K. Jiang, J. Phys. Chem. B 108, 2788, 2004.
4. X.L. Hu, Y. Zhu, J. Langmuir 20, 1521,2004.
5. C. L. Melcher, R. A. Manentem, J. S. Schweitzer, IEEE Trans. Nucl. Sci. 36, 1188, 1989.
6. C. L. Melcher, private communications 75, 1994.
7. D. Brown, R. H. Olsher, Y. Eisen, J. F. Odriguez, Nucl. Instrum. Methods Phys. Res. A 373, 139, 1996.
8. C. M. Bartle, R. C. Haight, Nucl. Instrum. Methods Phys. Res. A 422, 54, 1999.
9. V. Ryzhikov, L. Nagornaya, V. Volkov, V. Chernikov, O. Zelenskaya, Nucl. Instrum. Methods Phys. Res. A 486, 156, 2002.
10. M. Hojamberdiev, G. Zhu, Y. Xu, Mater. Res. Bull. 45, 2010.
11. J. Wang, Y. Xu, M. Hojamberdiev, J. Peng, G. Zhu,Mater. Sci. Eng. B 156, 2009.
12. H.-W. Liao, Y.-F. Wang, X.-M. Liu, Y.-D. Li, Y.-T. Qian,Chem. Mater. 12, 2000.
13. Mirabbos Hojamberdiev, Raghunath Kanakala, Olim Ruzimuradov, Yinglin Yan, Gangqiang Zhu, Yunhua Xu Optical Materials 34, 2012.

14. K. Polak, M. Niki, K. Nitsch, M. Kobayashi, M. Ishii, Y. Usuki and J. Jarolimerk, J. Lumin., 781,1997.
15. O.V. Rzhevskaya, D.A. Spasskiı, V.N. Kolobanov, V.V. Mikhaılin, L.L. Nagornaya, I.A. Tupitsina, B.I. Zadneprovskiı, Opt. Spectrosc. 104, 2008.
16. Y.A. Hizhnyi, S.G. Nedilko and T.N. Nikolaenko, Nucl. Instrum. Methods Phys. Res. A, 537, 2005.
17. Y. C. Kong, D.P.Yu, B. Zhang, W. Fang and S. Q. Feng, Appl. Phys. Lett. 78, 2001.
18. R. Chen, G.Z. Xing, J. Gao, Z. Zhang, T. Wu and H.D. Sun. Appl. Phy Lett. 95, 2009.
19. F. Chen, P. Huang, Y.J. Zhu, J. Wu, C.L. Zhang, D.X. Cui, Biomaterials, 32, 9031, 2011.
20. J.W. Stouwdam, Ph.D. Thesis, Faculty of Science and Technology, University of Twente, Enschede, The Netherlands, 2003.
21. C.S. Lim Mater. Chem. Phys. 131, 2012
22. D. Son, D.-R. Jung, J. Kim, T. Moon, C. Kim, B. Park,Appl. Phys. Lett. 90, 2007.
23. B. Gao, H. Fan and X. Zhang, S. Afr. J. Chem. 65, 2012.
24. Dhaval Modi, M. Srinivas, D.Tawde, K.V.R. Murthy, V. Verma and Nimesh Patel, J. Exp. Nanosci. http://dx.doi.org/10.1080/17458080.2014.899714, 2014.
25. Zawadzksi M. J AlloysCompd.451, 2008.
26. M.L.DosSantos, R.C.Lima, C.S.Riccardi, R.L.tranquilin, P.R.Bueno, J.A.Varela, E.Longo Material Leeters 62, 2008.

27. M.Srinivas, Dhaval Modi, Nimesh Patel, V.Verma and K.V.R.Murthy, Journal of Inorganic and Organometallic and. Polymer DOI 10.1007/s10904-014-0065-5, 2014.